The evolution of the electric field at a nonstationary perpendicular shock

Z. W. Yang,[1,2] Q. M. Lu,[1,2,a)] and S. Wang[1]
[1]*CAS Key Laboratory of Basic Plasma Physics, School of Earth and Space Sciences, University of Science and Technology of China, Anhui 230026, China*
[2]*State Key Laboratory of Space Weather, Chinese Academy of Sciences, Beijing 100190, China*

(Received 21 September 2009; accepted 30 November 2009; published online 29 December 2009)

Particle-in-cell simulations evidenced that supercritical, quasiperpendicular shocks are nonstationary and may suffer a self-reformation on the ion gyroscale. In this brief communication, we investigate the evolution of the electric field at a nonstationary, supercritial perpendicular shock. The contributions of the ion Lorentz, Hall, and electron pressure terms to the electric field are analyzed. During the evolution of the perpendicular shock, a new ramp may be formed in front of the old ramp, and its amplitude becomes larger and larger. At last, the new ramp exceeds the old one, and such a nonstationary process can be formed periodically. When the new ramp begins to be formed in front of the old ramp, the Hall term becomes more and more important. The electric field E_x is dominated by the Hall term when the new ramp exceeds the old one. The significance of the evolution of the electric field on shock acceleration is also discussed. © *2009 American Institute of Physics*. [doi:10.1063/1.3275788]

Collisionless shocks are of great interests since in the shock transition the bulk energy of the plasma is converted irreversibly into thermal energy.[1,2] According to θ_{Bn} (the angle between the shock normal and upstream magnetic field), shocks can be separated into two groups: quasiparallel shocks ($\theta_{Bn}<45°$) and quasiperpendicular shocks ($\theta_{Bn}>45°$). In quasiperpendicular shocks, the electric field in the shock transition region have great effects on ion acceleration.[3–6] When the electric field is sufficiently large, the reflected ions are accelerated by the mechanism of shock surfing acceleration (SSA); otherwise, the reflected ions are accelerated by the mechanism of shock drift acceleration (SDA). The acceleration efficiency of SSA and SDA is different for ions with different energies. Therefore, the electric field at quasiperpendicular shocks needs to be analyzed carefully. Recent investigation on magnetic reconnection demonstrated that on the ion inertial scale near the X point the ions are demagnetized while the electrons are frozen in the magnetic field, and the Hall term dominates the electric field. On the electron inertial scale, even the electrons are demagnetized, and the electric field is dominated by the off-diagonal electron pressure.[7,8]

Both particle-in-cell (PIC) and hybrid simulations clearly evidenced that supercritical, quasiperpendicular shocks are nonstationary and suffer a self-reformation process on the gyroscale of the incident ions.[9,10] During their reformation process, the width of the shock ramp is on the scale of ion inertial length and changes greatly. In this brief communication, a one-dimensional (1D) PIC code is used to study the evolution of the electric field at a nonstationary, supercritical, perpendicular shock, and the contributions of ion Lorentz, Hall and electron pressure terms to the electric field are analyzed.

The initial and boundary conditions in the 1D PIC simulation are identical to those already described in detail in Ref. 10; the shock is initiated by a magnetic piston (utilized current pulse). Briefly, the shock geometry is defined in the upstream frame: the shock propagates along the x axis and a static magnetic field is applied along the z axis. All dimensionless quantities are indicated by a tilde "~" and normalized as follows. The spatial coordinate $\tilde{x}=x/\Delta$, velocity $\tilde{v}=v/\omega_{pe}\Delta$, time $\tilde{t}=\omega_{pe}t$, electric field $\tilde{E}=eE/m_e\omega_{pe}^2\Delta$, and magnetic field $\tilde{B}=eB/m_e\omega_{pe}^2\Delta$. The parameters Δ, ω_{pe}, m_e, and e are, respectively, the numerical grid size, the electron plasma frequency, the electron mass, and the electric charge. All basic parameters are identical to those employed by Hada *et al.*:[11] plasma box size length $L_x=4096$, velocity of light $\tilde{c}=3$, and mass ratio $m_i/m_e=84$. Initially, the particle density is $n_e=n_i=50$ at each grid point. The electron/ion temperature ratio $T_e/T_i=1.58$ is chosen. The ambient magnetic field is $|\tilde{B}_0|=1.5$. The shock front is propagating in a supercritical regime with an average Mach number about ($M_A=5.24$), where $M_A=\tilde{V}_{\rm shock}/\tilde{V}_A$ is determined in the upstream frame; the Alfven velocity $\tilde{V}_A$ equals 0.16 and the shock propagating speed $\tilde{V}_{\rm shock}$ is the moving speed of the shock ramp. The shock ramp is defined as the position with peak $|\partial\tilde{B}_z^2/\partial x|$. For these initial conditions, the plasma parameters are summarized in Table I for both electrons and ions. The Larmor gyroradius in the table is calculated based on the thermal velocity.

The nonstationarity of the perpendicular shock can be demonstrated in Fig. 1, which shows the time evolution of the magnetic field $\tilde{B}_z$ from $\tilde{t}=900$ to 1550. The shock is propagating from the left to the right. At about $\tilde{t}=1200$, the shock ramp (the old ramp) is at about $\tilde{X}=5070$. Later at about $\tilde{t}=1350$, the relatively high percentage of reflected ions accumulated in the foot so that the foot amplitude becomes larger and larger, therefore a new ramp is formed. At about $\tilde{t}=1490$, the new ramp, which is around $\tilde{X}=5320$, exceeds

a)Electronic mail: qmlu@ustc.edu.cn.

TABLE I. Upstream plasma parameters defined for PIC simulations.

		Electrons	Ions
Thermal velocity	$\tilde{V}_{thx,y,z}$	0.2	0.017
Debye length	$\tilde{\lambda}_D$	0.2	0.16
Larmor gyroradius	$\tilde{\rho}_c$	0.4	2.91
Inertia length	$\tilde{c}/\tilde{\omega}_p$	3.0	27.5
Gyrofrequency	$\tilde{\Omega}_c$	0.5	0.006
Plasma frequency	$\tilde{\omega}_p$	1.0	0.11
Gyroperiod	$\tilde{\tau}_c$	12.55	1055.46
Plasma beta	$\tilde{\beta}$	0.0355	0.0225

the amplitude of the old ramp. Simultaneously, the old ramp downstream of the new ramp becomes weaker and weaker. The shock front is characterized by a self-reformation process with a cyclic period about $288\omega_{pe}^{-1} \approx 1.73\ \Omega_{ci}^{-1}$. The reformation of the shock front is due to the coupling between the "incoming" and "reflected" ions, which has been demonstrated by Hada *et al.*[11]

The evolution of the electric field in this nonstationary perpendicular shock is investigated in this brief communication. Assuming a two-fluid model for the plasma, the electric field can be obtained directly from the electron momentum equation without further approximation

$$\mathbf{E} = -\frac{\mathbf{V}_e \times \mathbf{B}}{c} - \frac{\nabla \cdot \underline{\mathbf{P}}_e}{en_e} - \frac{m_e}{e}\frac{d\mathbf{V}_e}{dt}. \tag{1}$$

Here $\mathbf{V}_e$ is the electron fluid velocity, $\mathbf{B}$ is the magnetic field, $\underline{\mathbf{P}}_e$ is the electron pressure tensor, c is the velocity of light, n_e is the electron density, m_e is the electron mass, and e is the electric charge. If we use the total current density $\mathbf{J}=e(n_i\mathbf{V}_i - n_e\mathbf{V}_e)$ (where $\mathbf{V}_i$ is the ion fluid velocity and n_i the ion density) and considering the 1D property of our simulation, the normalized Eq. (1) can be rewritten as

$$\tilde{\mathbf{E}} = -\frac{\tilde{n}_i}{\tilde{n}_e}\frac{\tilde{\mathbf{V}}_i \times \tilde{\mathbf{B}}}{\tilde{c}} + \frac{\tilde{\mathbf{J}} \times \tilde{\mathbf{B}}}{\tilde{c}\tilde{n}_e} - \frac{1}{\tilde{n}_e}\left(\frac{\partial \tilde{n}_e \tilde{T}_{exx}}{\partial \tilde{x}}\hat{\mathbf{e}}_x + \frac{\partial n_e \tilde{T}_{exy}}{\partial \tilde{x}}\hat{\mathbf{e}}_y + \frac{\partial \tilde{n}_e \tilde{T}_{exz}}{\partial \tilde{x}}\hat{\mathbf{e}}_z\right) - \frac{d\tilde{\mathbf{V}}_e}{d\tilde{t}}, \tag{2}$$

where $\tilde{T}_{exx} = \Sigma_{i=1}^{\tilde{n}_e}(\tilde{v}_{exi} - \tilde{V}_{exi})^2/\tilde{n}_e$, $\tilde{T}_{exy} = \Sigma_{i=1}^{\tilde{n}_e}(\tilde{v}_{exi} - \tilde{V}_{exi}) \times (\tilde{v}_{eyi} - \tilde{V}_{eyi})/\tilde{n}_e$, and $\tilde{T}_{exz} = \Sigma_{i=1}^{\tilde{n}_e}(\tilde{v}_{exi} - \tilde{V}_{exi})(\tilde{v}_{ezi} - \tilde{V}_{ezi})/\tilde{n}_e$ are components of the electron kinetic temperature.[12] $\hat{\mathbf{e}}_x$, $\hat{\mathbf{e}}_y$, and $\hat{\mathbf{e}}_z$ are unit vectors. The first, second, third, and fourth terms in the right of Eq. (2) are ion Lorentz term, Hall term, electron pressure term, and electron inertial term, respectively. All of the physical quantities in the right of Eq. (2) can be obtained from the PIC simulation by a statistical method. We choose three typical shock profiles at three different times within one shock self-reformation cycle (from $\tilde{t}$=912 to

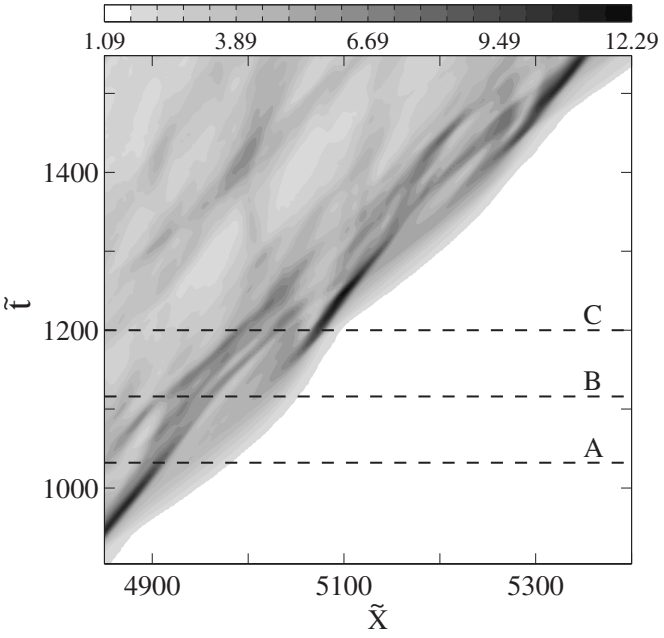

FIG. 1. The time evolution of $\tilde{B}_z$ vs $\tilde{X}$. Dashed lines A, B, and C indicate the shock profiles that are chosen in Figs. 2–4 within one cyclic self-reformation of the shock front.

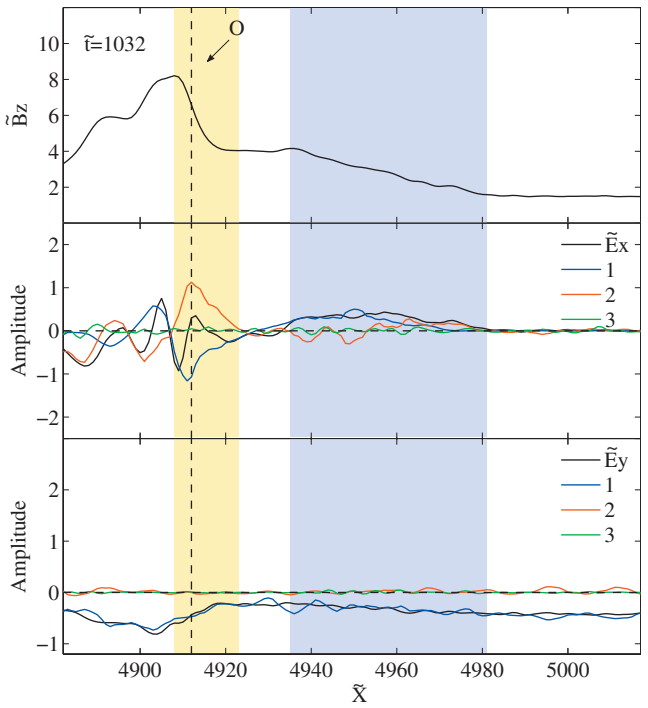

FIG. 2. (Color) Spatial profiles of the magnetic field $\tilde{B}_z$ (top panel), electric fields $\tilde{E}_x$ (middle panel), and $\tilde{E}_y$ (bottom panel) in the vicinity of the shock ramp at $\tilde{t}$=1032, corresponding to line A in Fig. 1. The additional curves indicate the contributions to $\tilde{E}_x$ and $\tilde{E}_y$ of the terms on the right of Eq. (2), ion Lorentz term (line 1), Hall term (line 2), and electron pressure gradients term (line 3). "O" denotes the position of the old ramp during one reforming cycle, and the yellow and cyan highlight the regions where magnetic field is steepening in the vicinity of ramp and foot, respectively. The electric field is calculated in the shock-rest frame.

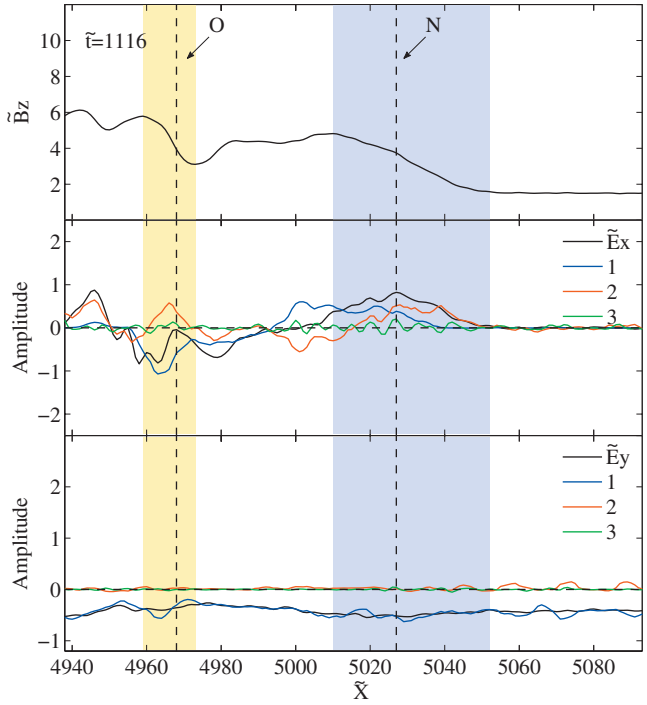

FIG. 3. (Color) Spatial profiles of the magnetic field $\tilde{B}_z$ (top panel), electric fields $\tilde{E}_x$ (middle panel), and $\tilde{E}_y$ (bottom panel) in the vicinity of the shock ramp at $\tilde{t}=1116$, corresponding to line B in Fig. 1. The additional curves are as in Fig. 2. "O" and "N" denote positions of the old and new ramps during one reforming cycle, respectively, and the yellow and cyan highlight the regions where magnetic field is steepening in the vicinity of old ramp and new ramp, respectively. The electric field is calculated in the shock-rest frame.

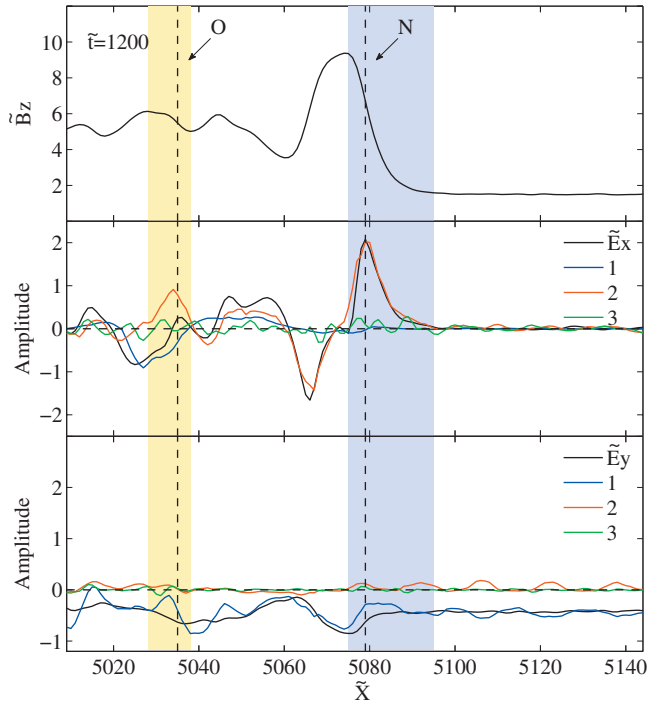

FIG. 4. (Color) Spatial profiles of the magnetic field $\tilde{B}_z$ (top panel), electric fields $\tilde{E}_x$ (middle panel), and $\tilde{E}_y$ (bottom panel) in the vicinity of the shock ramp at $\tilde{t}=1200$, corresponding to line C in Fig. 1. The additional curves are as in Fig. 2. "O" and "N" denote positions of the old and new ramps during one reforming cycle, respectively, and the yellow and cyan are as in Fig. 3. The electric field is calculated in the shock-rest frame.

1200), and then analyze separately the corresponding contributions of ion Lorentz, Hall, and electron pressure terms to the $\tilde{x}$ and $\tilde{y}$ components of the electric field $\tilde{\mathbf{E}}$. Although our 1D PIC simulation is performed in the upstream frame, the electric field in the following text is calculated in the shock-rest frame. At the same time, the $\tilde{z}$ component of $\tilde{\mathbf{E}}$ is not shown because the amplitude of $\tilde{E}_z$ is smaller than the other components by two orders of magnitude.

Figure 2 shows the snapshots of shock profile $\tilde{B}_z$, $\tilde{E}_x$, and $\tilde{E}_y$ at $\tilde{t}=1032$. At this time, the shock front includes a ramp and a foot in front of the ramp. The width of the shock ramp, which is measured from the beginning point of magnetic steepening to the maximum point of the magnetic overshoot,[13] is about 15. The position of the ramp (denoted by "O") is at $\tilde{x}=4912$. The electric field $\tilde{E}_x$ (black line) has a positive value at the shock foot. It is dominated by the ion Lorentz term, and the other two terms are not important. However, near the shock ramp, the electric field $\tilde{E}_x$ changes greatly. Both the ion Lorentz and Hall terms are important, and the electron pressure term is negligible. For the electric field $\tilde{E}_y$, the ion Lorentz term always dominates the electric field $\tilde{E}_y$, and the Hall term is negligible.

Figure 3 shows the snapshots of the shock profile $\tilde{B}_z$, $\tilde{E}_x$, and $\tilde{E}_y$ at $\tilde{t}=1116$. At this time, the amplitude of the old ramp (denoted by "O") is decreasing, and the width of the old ramp is about 14. Simultaneously, a new ramp (denoted by "N") appears and its amplitude reaches at about 60% of the old ramp. The width of the new ramp is about 42. Now, the electric field $\tilde{E}_x$ has a positive value at the new ramp. The Hall term at the new ramp becomes more and more important, and it is comparable with the ion Lorentz term. While the electric field $\tilde{E}_x$ at the old ramp is decreasing, it also changes greatly while both the ion Lorentz and Hall terms are important. For the electric field $\tilde{E}_y$, similar to Fig. 2, the ion Lorentz term always dominates the electric field $\tilde{E}_y$, and the Hall term is negligible.

Figure 4 shows the snapshots of shock profile $\tilde{B}_z$, $\tilde{E}_x$, and $\tilde{E}_y$ at $\tilde{t}=1200$. The amplitude of the new ramp has already overcome the old one. The widths of the old and new ramps are about 10 and 20, respectively. Different from the above results, near the new shock ramp, because its width becomes very small, the Hall term now dominates the electric field $\tilde{E}_x$ and other terms are negligible.

In this brief communication, we use a 1D PIC simulation to study the evolution of the electric field at a nonstationary perpendicular shock. At the same time, we separate the electric field into ion Lorentz, Hall, and electron pressure terms, and their importance is evaluated. The ion Lorentz and Hall terms are two important contributions to the electric field. For the electric field E_x, after the new shock ramp is formed, the Hall term becomes more and more important with the

increase of the new ramp. When the new ramp exceeds the old ramp, its width is very small. It is comparable with or even smaller that the ion inertial length, and the Hall term dominates the electric field E_x. At that time, the electric field E_x dominated by the Hall term is obviously larger than that at other times. As pointed previously by Yang *et al.*,[6] at that time the SSA, where the particles are reflected mainly due to the electric field E_x, is an important mechanism to accelerate the reflected ions. Therefore, the contribution of the Hall term to the electric field has important significance on SSA acceleration at quasiperpendicular shocks. For the electric field E_y, the ion Lorentz term is always more important that other terms.

Recently, the ion-to-electron mass ratio has been demonstrated to have great influence on the structures of the quasiperpendicular shock. If a real ion-to-electron mass ratio is used, a modified two-stream instability on the electron inertial scale may be unstable at the foot of the shock,[14] and on this scale the electron pressure term may become important. Simultaneously, two-dimensional PIC simulations found that a supercritical quasiperpendicular shock may be emitted large-amplitude whistler waves,[15] which may change the structures of the shock. Their effects on the electric field at a quasiperpendicular shock also need to be evaluated, which is our future investigation.

We thank Dr. Bertrand Lembège for the useful discussion.

This research was supported by the National Science Foundation of China, Grant Nos. 40874075, 40725013, 4094093, and the Chinese Academy of Sciences, Grant No. KJCX2-YW-N28.

[1] B. Lembège, J. Giacalone, M. Scholer, T. Hada, M. Hoshino, V. Krasnoselskikh, H. Kucharek, P. Savoini, and T. Terasawa, Space Sci. Rev. **110**, 161 (2004).
[2] D. Burgess, E. A. Lucek, M. Scholer, S. D. Bale, M. A. Balikhin, A. Balogh, T. S. Horbury, V. V. Krasnoselskikh, H. Kucharek, B. Lembège, E. Möbius, S. J. Schwartz, M. F. Thomsen, and S. N. Walker, Space Sci. Rev. **118**, 205 (2005).
[3] A. S. Lipatov and G. P. Zank, Phys. Rev. Lett. **82**, 3609 (1999).
[4] K. Nishimura, H. Matsumoto, H. Kojima, and S. P. Gary, J. Geophys. Res. **108**, A51182 (2003).
[5] V. D. Shapiro and D. Üçer, Planet. Space Sci. **51**, 665 (2003).
[6] Z. W. Yang, Q. M. Lu, B. Lembège, and S. Wang, J. Geophys. Res. **114**, A03111, doi:10.1029/2008JA013785 (2009).
[7] V. M. Vasyliunas, Rev. Geophys. **13**, 303, doi:10.1029/RG013i001p00303 (1975).
[8] P. L. Pritchett, J. Geophys. Res. **106**, 3783, doi:10.1029/1999JA001006 (2001).
[9] X. Yuan, I. H. Cairns, L. Trichtchenko, R. Rankin, and D. W. Danskin, Geophys. Res. Lett. **36**, L05103, doi:10.1029/2008GL036675 (2009).
[10] B. Lembège and P. Savoini, Phys. Fluids B **4**, 3533 (1992).
[11] T. Hada, M. Oonishi, B. Lembège, and P. Savoini, J. Geophys. Res. **108**, 1233, doi:10.1029/2002JA009339 (2003).
[12] H. Heinz, W. Paul, and K. Binder, Phys. Rev. E **72**, 066704 (2005).
[13] N. Shimada and M. Hoshino, J. Geophys. Res. **110**, A02105, doi:10.1029/2004JA010596 (2005).
[14] M. Scholer, I. Shinohara, and S. Matsukiyo, J. Geophys. Res. **108**, 1014, doi:10.1029/2002JA009515 (2003).
[15] B. Lembège, P. Savoini, P. Hellinger, and P. M. Tràvnìcek, J. Geophys. Res. **114**, A03217, doi:10.1029/2008JA013618 (2009).